

Mechanotransduction through the cytoskeleton

YINON SHAFRIR¹ AND GABOR FORGACS²

¹Department of Physics, Clarkson University, Potsdam, New York 13676; and ²Department of Physics and Biology, University of Missouri, Columbia, Missouri 65211

Received 12 October 2001; accepted in final form 22 October 2001

Shafir, Yinon, and Gabor Forgacs. Mechanotransduction through the cytoskeleton. *Am J Physiol Cell Physiol* 282: C479–C486, 2002; 10.1152/ajpcell.00394.2001.—We constructed a model cytoskeleton to investigate the proposal that this interconnected filamentous structure can act as a mechano- and signal transducer. The model cytoskeleton is composed of rigid rods representing actin filaments, which are connected with springs representing cross-linker molecules. The entire mesh is placed in viscous cytoplasm. The model eukaryotic cell is submitted to either shock wave-like or periodic mechanical perturbations at its membrane. We calculated the efficiency of this network to transmit energy to the nuclear wall as a function of cross-linker stiffness, cytoplasmic viscosity, and external stimulation frequency. We found that the cytoskeleton behaves as a tunable band filter: for given linker molecules, energy transmission peaks in a narrow range of stimulation frequencies. Most of the normal modes of the network are spread over the same frequency range. Outside this range, signals are practically unable to reach their destination. Changing the cellular ratios of linker molecules with different elastic characteristics can control the allowable frequency range and, with it, the efficiency of mechanotransduction.

intracellular signal transduction; computational model; mechanical energy transfer

REGULATION OF VARIOUS CELL FUNCTIONS by mechanical forces has by now been amply demonstrated (for reviews, see Refs. 5–7, 21, 33, and 41). Because all cells of an organism are exposed to external forces, it may not be surprising that cells sense these forces. What is surprising is the fact that physical factors control biological processes such as cell differentiation, proliferation (35), gene expression (19, 29, 35), and, in particular, signal transduction, the subject of the present work, that are believed to be regulated by specific biochemical molecules and reactions. The amplitude and frequency of Ca²⁺ waves induces differential activation of transcription factors (8). Shear stress activates G proteins in a magnitude- and rate-dependent manner (13, 14). The extent of tyrosine phosphorylation depends on the frequency of the cyclic force applied to integrin receptors (39, 44). It seems that mechanical and biochemical signaling effects converge on the molecular scale.

Despite recent efforts, the cellular mechanism of mechanically induced signal transduction is largely

unknown. It is widely accepted that such signaling pathways start with mechanosensitive cell surface receptors (1) like integrins, cell adhesion molecules (18, 23, 25, 38, 39, 44), or stretch-activated ion channels (30, 40). The conformational change in these receptors then activates second messengers and/or induces a cascade of enzymatic reactions, which may involve a large number of downstream players. How these molecules carry out their spatial and temporal functions is still a mystery.

It has been recognized that mechanical signaling involves the cytoskeleton (17). Inhibition of actin stress fiber development blocks fluid shear-induced gene expression in osteoblasts (35). Integrin-mediated signaling processes are interrupted by cytoskeletal disassembly (38, 44). In the absence of cytoskeletal attachment, cadherins do not function as cell adhesion molecules and do not transmit mechanical signals (15, 34). Oscillatory mechanical stimulation of chick osteoblasts increases the levels of osteopontin provided the actin cytoskeleton is intact (48). Mechanical stretching of rat vascular smooth muscle cells induces extracellular signal-regulated kinase by activation of Rho kinase. A precondition for this to take place is an uninterrupted microfilament network (32). More direct evidence of the importance of coupling of mechanical forces and the cytoskeleton is the remarkable role microtubules play during mitosis. Tension in the kinetochores is crucial to the normal progression of anaphase. Without tension, anaphase is delayed. When tension is restored through mitotic forces or micromanipulation, cell division proceeds (31).

Because of its interconnected structure, the cytoskeleton is an obvious candidate for mechanotransduction (10, 23). However, its role in signaling also is secured by the fact that it accommodates the numerous signaling molecules (e.g., kinases, phosphatases) a cell possesses (17, 27, 44).

The specific relationship between cytoskeletal structure, cellular mechanics, and intracellular signaling is unclear. Proposals vary from continuum models (9) to tensegrity (16) and percolation structures (10). Recently, it was suggested that a specific way the cytoskeleton may participate in signal transduction is by furnishing tracks on which signaling agents can move

Address for reprint requests and other correspondence: Y. Shafir, Laboratory of Experimental and Computational Biology, National Institutes of Health, Bethesda, MD 20892-5677 (E-mail: yinon@nih.gov).

The costs of publication of this article were defrayed in part by the payment of page charges. The article must therefore be hereby marked "advertisement" in accordance with 18 U.S.C. Section 1734 solely to indicate this fact.

(even) without molecular motors. It was shown that this mechanism could significantly improve the efficiency of signal transfer (46).

If indeed mechanical force propagation through the cytoskeleton can provide biological specificity, as numerous experiments have shown, the filaments must be able to transmit mechanical energy with high reliability. This energy transfer, when sensed by signaling molecules anchored to the cytoskeleton, may change their molecular conformation, thus providing a specific contribution to intracellular signaling pathways.

Motivated by the possible role of mechanical processes in intracellular signaling, in the present work we have studied the energy transfer properties of the cytoskeleton using computer simulations. Our basic assumption was that the intracellular filamentous mesh is imbedded in the highly viscous cytoplasm; thus it is a source of energy dissipation. Because in most cases cells are exposed to intermittent mechanical perturbations (14, 22, 30, 44), we subjected the receptors of our model cells to oscillatory forces and asked the question, what ratio of the supplied energy reaches the nucleus? We have shown that at physiological filament concentrations and realistic physical (i.e., viscoelasticity) parameter values, the energy transfer ratio peaks in the 0.1- to 10-Hz frequency range. This finding is consistent with the results of recent experiments probing the mechanotransductive properties of the cytoskeleton (44).

MATERIALS AND METHODS

Model cytoskeleton. As a model for the cell, we used a cube with sides of 5 μm , centered inside another cube with sides of

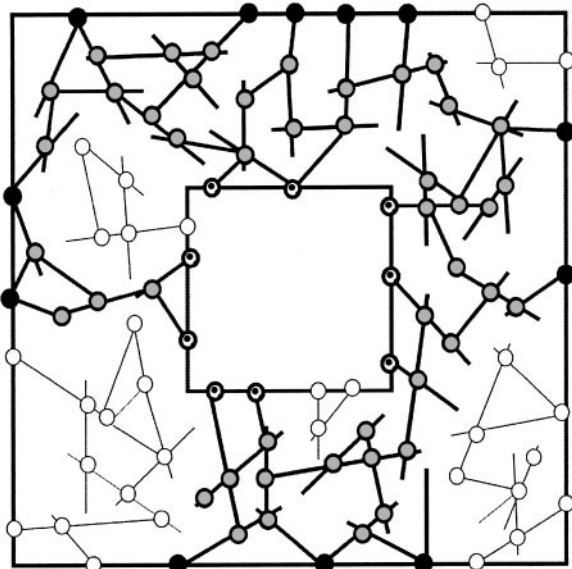


Fig. 1. The model cell: two-dimensional projection of the model cell with a schematic representation of the cytoskeletal network. Filaments that form an uninterrupted path from the cell surface to the nucleus are denoted by heavy lines. Filaments that do not belong to this uninterrupted percolation cluster are represented by thin lines. Filled and dotted circles represent intersection points of percolating filaments with the cell and nuclear boundaries, respectively. Shaded circles represent elastic cross-linkers. See text for details.

10 μm (Fig. 1). The former cube represents the nucleus. Our model cytoskeleton consists of rigid rods connected through springs. The rods may represent various cytoskeletal filaments if their diameter is chosen appropriately. The cytoskeleton of a typical eukaryotic cell comprises three types of filaments: actin filaments, microtubules, and intermediate filaments. These filaments are cross-linked (36, 47). They form a globally interconnected network that extends from the cell membrane to the nuclear wall. In this work, to simplify the simulations, we introduced only one kind of filament. We used rods of 8 nm in diameter (i.e., model actin filaments) with lengths between 0.5 and 1.5 μm . Each rod was characterized by six parameters that describe its location in space: Cartesian coordinates for one of the end points, the rod length, and two angles determining its orientation. The random network of rods was generated in a computer, using independent random numbers for each of the six parameters.

While constructing the network, the following rules were observed. Two rods could not penetrate each other. Once two filaments were within minimal distance of one another (i.e., within their soft core = 0.2 μm), cross-linking springs were attached to them at the points of shortest distance. These springs might represent actin cross-linking proteins such as filamin. Rods were restricted to the space between the nucleus and the cell surface. Rods that crossed either the cell membrane or the nuclear wall were “chopped” at the point of intersection with these planes.

To mimic the interconnected character of the cytoskeleton, the concentration of the model filaments was chosen to exceed the percolation threshold (46). The concept of percolation, widely utilized in physical and engineering sciences (42), refers to the transition when by increasing the concentration of certain randomly distributed structural elements (i.e., rods), a continuous interconnection between the boundaries of the system in which they reside is formed (10).

Equations of motion. Once a network was constructed, a mechanical signal was applied in the form of sinusoidal mechanical torque to the rods anchored to the cell membrane. This corresponded to a situation recently realized experimentally by Maksym et al. (22). These authors oscillated small magnetic beads bound specifically to integrin receptors. Because integrins are connected to the cytoskeleton, they were able to transmit mechanical energy to the network and study its viscoelastic response. In our system, because of the springs, the signal propagated through the network. We were eventually interested in the effect of this mechanical signal on the filaments attached to the nuclear wall. To follow the signal at any point in time, we had to solve two sets of linear differential equations for each rod. One is the linear Newtonian set of equations

$$\frac{dp_i}{dt} = \left(\sum \mathbf{F} \right)_i - \mathbf{F}_{d,i}, \quad i = x, y, z \quad (1)$$

Here, p_i , $(\sum \mathbf{F})_i$, and $\mathbf{F}_{d,i}$ are the i th components ($i = x, y, z$) of the rod's center of mass momentum, the sum of all forces exerted on the rod by the connected springs in the i th direction, and the drag force, respectively. For the drag force

$$\mathbf{F}_d = -\frac{4\pi\eta l}{\ln\left(\frac{2l}{d}\right) + \frac{1}{2}} \mathbf{v}_\perp + \frac{2\pi\eta l}{\ln\left(\frac{2l}{d}\right) - \frac{1}{2}} \mathbf{v}_\parallel$$

where l is the length of the rod, d is its diameter, and η is the viscosity of the surrounding cytoplasm. \mathbf{v}_\perp and \mathbf{v}_\parallel are the velocity components perpendicular and parallel, respectively, to the length of the rod. The above expression is valid in the limit $l/d \gg 1$ (2).

The rotational motion is determined by the standard Euler equations (12). To simplify the equations, it is useful to write them for a particular rod in the body reference frame of the rod in which the momentum of inertia tensor is diagonal

$$\begin{aligned}\frac{dJ_x}{dt} &= N_x + (I_y - I_z)\omega_y\omega_z - B_{d_x}\omega_x \\ \frac{dJ_y}{dt} &= N_y + (I_z - I_x)\omega_x\omega_z - B_{d_y}\omega_y \\ \frac{dJ_z}{dt} &= N_z + (I_x - I_y)\omega_x\omega_y - B_{d_z}\omega_z\end{aligned}\quad (2)$$

Here, J_i , N_i , ω_i , and B_{d_i} are the respective i th components of the angular momentum vector, the applied torque about the point of rotation, the angular velocity vector, and the rotational frictional drag. I_i is the moment of inertia about the i th principle axis. For the rods that are part of the bulk or attached to the nucleus, the applied torque is merely the total torque exerted by the springs, whereas for the rods that are attached to the membrane, it includes the stimulation torque. If we choose the z -axis of the body reference frame to align with the length of the rod, then for the frictional drag

$$B_{d_x} = B_{d_y} = \frac{\pi\eta l^3}{3 \left[\ln\left(\frac{2l}{d}\right) - \frac{1}{2} \right]}$$

$$B_{d_z} = \frac{2}{3} \pi\eta l d^2$$

These expressions are valid in the limit $l/d \gg 1$ (2). If we further assume no initial rotation, then because of the condition $l/d \gg 1$, we can ignore rotation around the z -axis ($B_{d_z} \approx 0$ and $I_x = I_y$). Equations 1 and 2 apply to each filament. The simulations are somewhat simplified by the fact that for the rods anchored to either the nucleus or the membrane, there is no need to solve the linear equations of motion.

Because in the present case the linear Eqs. 1 are strongly coupled to the rotational Eqs. 2 (through the forces F_i caused by springs in Eqs. 1, which give rise to the torques N_i in Eqs. 2), the simultaneous solution of the equations of motion is highly nontrivial. As a consequence, standard numerical methods for solving sets of differential equations are impractical to use in the present large-scale simulations. They are either too simple, leading to numerical error increasing with time (e.g., the Euler method), or too cumbersome and time consuming (e.g., Runge-Kutta IV). As a reasonable compromise, we used the leapfrog algorithm (4), which is fast enough to handle vast amounts of equations, yet error propagation is proportional to the square of the time step used in the simulation.

Computer. Calculations were performed on Intel 400-MHz Celeron machines. CPU time for one typical run (including the construction of the model cytoskeleton with 25,000–35,000 rods and the solution of the equations of motion for a given filament configuration and 20-s simulated time) was about 48 h.

RESULTS

A mechanical signal can be initiated in many ways and have many forms. In this work we concentrated on two types of mechanical signals. The first was a shock wave in which a mechanical stress was applied to the membrane-anchored filaments (MAFs) for a very brief

period of time (instantaneously). The second was a sinusoidal stimulation of MAFs for a set amount of time. In both cases the ratio of the total energy on the nucleus and the total energy on the membrane was calculated as a measure of the efficiency of the network as an information transmitting system.

In these simulations we analyzed the influence of three major parameters on signal propagation: the cytoplasmic viscosity, the stiffness of the cross-linking molecules, and, in the case of a continuous sinusoidal signal, the external signal frequency. The value of cytoplasmic viscosity depends on many factors, including the level of cytoskeleton polymerization. We used three values: η_w , $10\eta_w$, and $100\eta_w$, where η_w is the viscosity of water (1 cP). For the stiffness of cross-linkers, we used 100, 1,000, and 10,000 pN/ μ m. These parameter values were dictated by data found in the literature (3, 20, 26, 28). The response for continuous stimulation was measured over frequencies ranging from 0.1 to 500 rad/s.

Shock wave stimulus. The main characteristics of the energy distribution in a system subjected to an instantaneous stimulation are summarized in Fig. 2. The initial signal was achieved by compressing the springs attached to the MAFs to a certain fraction of their equilibrium lengths. (The results are virtually independent of the initial compression.) The stiffness of the springs in all cases was set to 1,000 pN/ μ m. As expected, the energy on the nucleus decreased with increasing cytoplasmic viscosity. In all cases the signal on the nucleus attained its maximum amplitude relatively fast (~ 3 s). This conclusion is not sensitive to filament concentration once beyond the percolation threshold, where cytoplasmic filaments form an interconnected network, which extends from the cell membrane to the nucleus (46). Most of the simulations were performed at the concentration of model actin filaments of 1.56 mg/ml, corresponding to 25,000 filaments. (At such concentrations, results depend very little on the number of rods, as shown in Fig. 3.) The ratio of the energies ranges from $<1\%$ at

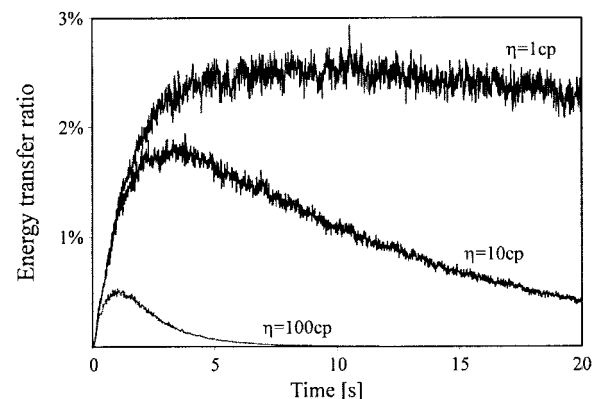


Fig. 2. Response to instantaneous shock wave stimulus as indicated by energy transfer ratios. Spring stiffness in all cases was set to 1,000 pN/ μ m. As expected, the energy on the nucleus decreases with increasing cytoplasmic viscosity (η). In all cases, the signal on the nucleus attains maximum amplitude relatively fast (~ 3 s).

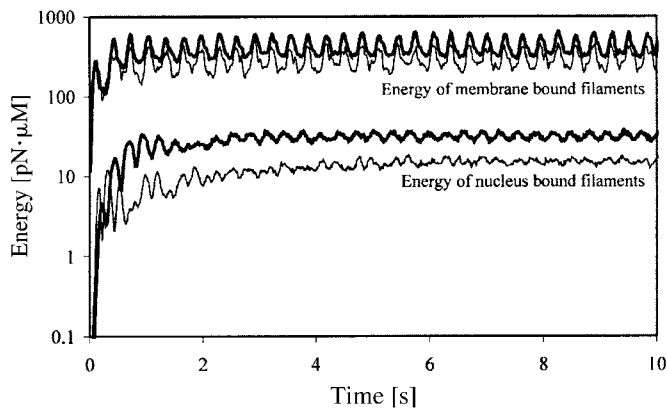


Fig. 3. Response to continuous stimulation at 2 different network concentrations. The differences between energy transfer ratios of a network consisting of 35,000 filaments (thick line) and a network of 25,000 filaments (thin line) are insignificant.

the highest viscosity to 3% at the lowest viscosity. However, one must take into account that because of the geometry of our system, the number of filaments connected to the membrane was four times larger than the number of filaments connected to the nucleus. Hence, the energy ratio per filament ranged between 4 and 12%.

Continuous stimulation. Matters became more complex when the system was subjected to a sinusoidal stimulation. Two characteristic energy patterns are shown in Fig. 4. In Fig. 4A, the system was excited with a frequency of 10 rad/s (~ 1.6 Hz). The energies at both the membrane and the nucleus settled around an equilibrium value with very little fluctuations. In Fig. 4B, the signal had a frequency of 0.1 rad/s (~ 0.016 Hz) and lasted 100 s. In this case it appeared as if no steady state was attained. Eventually the system stabilized (results not shown), but the fluctuations around the average remained significant. The system followed the signal on both the membrane and the nucleus, with noticeable shift in phase. When the stimulation ended, the system exhibited a shock wave-like response.

Effect of intrinsic intracellular properties. In Fig. 5, we calculated the energy transfer ratio as a function of external stimulation frequency, stiffness of linkers, and cytoplasmic viscosity. In all cases there was a distinct peak, where the ratio reached a maximum. The location of this peak depended on cross-linker stiffness and apparently was insensitive to cytoplasmic viscosity. Furthermore, the width of the peak increased, whereas its height decreased, with stiffness. Some of these findings are easy to interpret. In the case of low-frequency stimulation, the cytoskeleton had enough time to rearrange itself to adjust locally to a new low-energy configuration. Thus the system was able to absorb a significant fraction of the input energy, allowing only a small amount to arrive at the nucleus. At very high stimulation frequencies, the springs effectively froze and behaved as rigid objects; again very little energy was transmitted through the network. Between these extreme situations the transfer ratio

reached a maximum value that, as expected, decreased with viscosity. These results show that with stiffer cross-linkers, the range of frequencies at which a signal can get through is somewhat larger, whereas its intensity is comparably smaller.

Another intrinsic property of the cytoskeletal network is demonstrated in Fig. 6. An interconnected network that contains elastic components has intrinsic frequencies called eigenfrequencies, or normal modes. Once the network vibrates, the oscillations of its elements are given as a linear combination of the normal modes. For the instantaneous displacement $\Delta l(t)$ of a particular spring from its original length l , one obtains $\Delta l = \sum a_i \cos(\omega_i t)$, where a_i is the amplitude or weight of the i th eigenfrequency ω_i and summation is meant over all normal modes. By means of Fourier analysis, it is possible to determine the eigenfrequencies and their relative amplitudes (see Fig. 6). The physical importance of this spectrum is that if an external stimulation matches one of the eigenfrequencies, the system will oscillate with minimal energy loss (i.e., with maximum power in Fig. 6). Indeed, as demonstrated by Fig. 6, most eigenfrequencies are in the same range where the energy transfer reached its maximum (compare with Fig. 5).

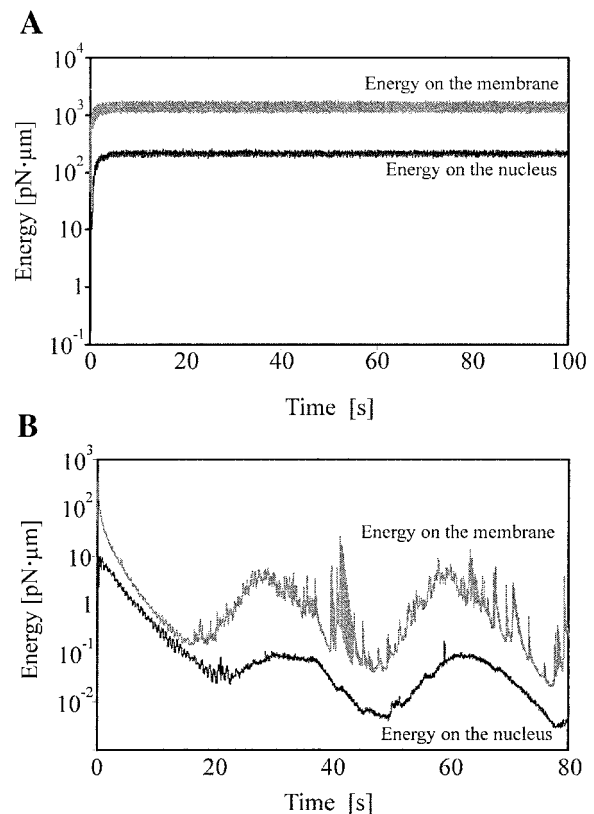


Fig. 4. Energy patterns as a result of 2 different driving frequencies. A: at an excitation frequency of 10 rad/s, the energy of rods connected to the nucleus and the energy of rods connected to the membrane reach their equilibrium values after 3 s. B: at an excitation frequency of 0.1 rad/s, the energies acquire a somewhat periodical pattern only after 40 s.

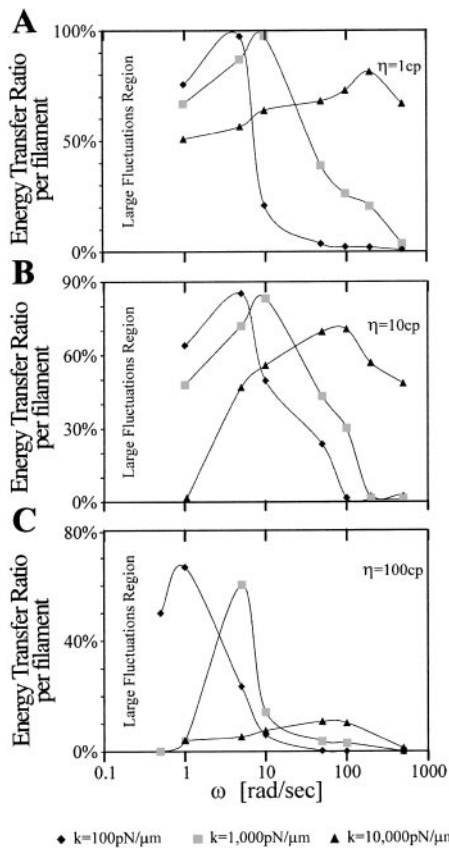


Fig. 5. Energy transfer ratio per filament as a function of the external driving frequency, spring constant (k), and viscosity. *A*: low-viscosity regime ($\eta = 1$ cP). *B*: intermediate-viscosity regime ($\eta = 10$ cP). *C*: high-viscosity regime ($\eta = 100$ cP). As expected, the transfer ratio decreases with viscosity. The frequency band width increases, whereas the transfer ratio decreases, with spring constant. The x -axis is logarithmic and common to all graphs. Ratios are shown only for frequencies where a distinct flat level for the energy as a function of time was attained (compare with Fig. 4).

DISCUSSION

It is widely accepted that mechanical forces are directly involved in cell function regulation. Nevertheless, the role of mechanical processes in intracellular signaling is still being questioned. This is due to two major limitations associated with mechanical signals. First, such signals are easily degraded because of rapid energy dissipation. Secondly, to achieve specificity, mechanical signals eventually have to regulate biochemical reactions. How this conversion process takes place is still obscure.

It has been demonstrated amply that in many mechanical and biochemical processes, the cytoskeleton plays an essential role. For example, the cytoskeleton is responsible for cell shape regulation and locomotion (mechanical effects) and at the same time provides docking sites for conventional signaling molecules (chemical effect). This duality in the cytoskeleton's role makes it an ideal candidate for a cellular mechanochemical conversion apparatus.

In the present study, using a simplified model we demonstrated that by exploiting the interconnected

character of the cytoskeleton, a mechanical signal can traverse the entire gap between the membrane and the nucleus in a relatively short time without being completely degraded. Furthermore, by tuning the signal frequency to the network's intrinsic feature, the vibrational normal modes, biochemical reactions could be differentially affected.

We started with a random network consisting of stiff rods and elastic springs that represent cytoskeletal filaments and cross-linking molecules, respectively. We applied two different types of mechanical signals at the cell membrane: a shock wave and a continuous sinusoidal stimulation. We compared the output energy on the nucleus with the input energy on the

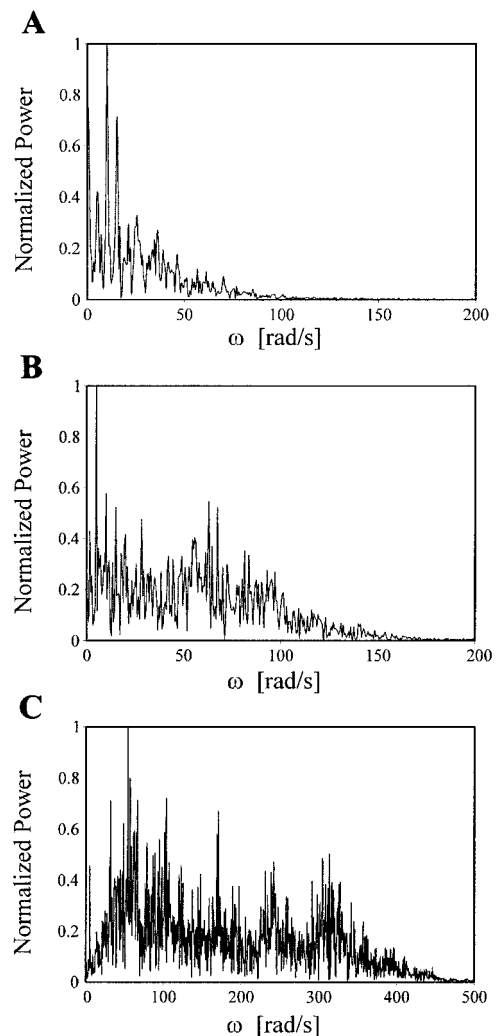


Fig. 6. Normalized power spectrum for different spring constants. The viscosity in all graphs is 10 cP, and the driving frequency is 5 rad/s. The spring constants were 100 (*A*), 1,000 (*B*), and 10,000 pN/ μ m (*C*). The oscillations of the spring can be written as $\Delta l = \sum a_i \cos(\omega_i t)$ (see text). Each peak in the graph represents the relative value of the Fourier coefficients $(a_i/a_{\max})^2$, where a_{\max} is the coefficient with the largest value. Maximal energy transfer occurs when the external driving frequency corresponds to a sharp peak in the power spectrum. (Although these graphs were obtained for a particular value of the driving frequency, the location of the eigenfrequencies does not depend on that choice.)

membrane. We then looked at how this ratio changed with the physical properties of the network-signal system: viscosity, cross-linkers elasticity, and signal frequency.

When the network was perturbed by a shock wave at the filament concentration used in this work (1.56 mg/ml, corresponding to 25,000 “actin-like filaments”), the signal reached its maximal value at the nucleus within 3 s after initiation. This finding is independent of cytoplasmic viscosity or initial signal amplitude. When continuous stimulation was considered, different energy profiles were observed. Rather than achieving a distinct peak, as was the case with a shock wave, above a certain driving frequency the energy profile at the nucleus reached a steady-state level with few fluctuations. Again, it took the system about 3 s to reach this state. The energy loss was apparent but not detrimental to the integrity of the signal. Below a certain frequency, the system stabilized only after a much longer transient time, the fluctuations around the average remained significant and the energy transferred to the nucleus was comparatively small (see Figs. 4 and 5).

Our results are consistent with a number of recent experimental findings, and some of our conclusions could be explored experimentally. Numerous investigators have found that cells are most responsive to sinusoidal stimulation within a narrow range of frequencies between 0.1 and 10 Hz (43–45). In our simulation, the highest energy transfer ratio was achieved in this exact frequency range (provided the spring constant was between 100 and 1,000 pN/ μm). The mechanical properties of the linker molecules (i.e., springs) strongly influence the width of this range. The stiffer the links, the wider the range. [The values of cross-linker stiffness and cytoplasmic viscosity used in the present simulations correspond to measurements cited in the literature (3, 20, 26, 28).] Thus the cytoskeleton effectively behaves as a “tunable band-pass filter:” for given linker molecules, the signals with frequencies outside a characteristic range are unable to reach their destination. Changing the cellular ratios of linker molecules with different elastic constants (α -actinin, filamin, plectin, etc.) can control the allowable frequency range and, with it, the efficiency of mechanical signal propagation.

The normal modes of our model cytoskeleton in general change with alterations in its architecture. However, our networks are random and well above the percolation threshold. Thus their physical properties, in particular normal modes, change little with configurational modifications, as long as the elastic characteristics of the linkers do not change (46). We have shown that for our networks, most of the normal modes are spread over the same frequency range where energy transduction is the most efficient (see Fig. 6). In a true cell, controlled cytoskeletal modifications (e.g., in the case of locomotion, cell division, etc.) may provide another mechanism to select the “right signals at the right time.”

A mechanical signal eventually must be translated into a biochemical reaction. Because many signaling molecules reside on the cytoskeleton (17, 27, 44), it is reasonable to assume that mechanical stimulation can activate some of them. Every signaling molecule has a characteristic activation rate. If the activation rate of a specific molecule matches the normal modes of the system, the probability of it being activated is the highest. The normal modes of the cytoskeletal mesh can be determined and then appropriately tuned by modifying the properties of the cross-linkers. For this, the motion of a particular segment of the network has to be followed with a high-speed camera. [Work along these lines already has been performed by Prahlad et al. (37), who monitored shape changes of individual intermediate filaments in living cells.] Fourier transformation of the amplitude of the vibrational motion, as explained earlier, provides the eigenfrequencies.

In Fig. 7, we demonstrate how energy transduction through the cytoskeleton could trigger or facilitate specific biochemical reactions. Energy transfer along the filaments causes their displacement. This may allow signaling molecules loosely bound to the cytoskeleton to approach and thus react with each other.

Our model is an oversimplified description of intracellular mechanical signal/energy transduction. Because of finite computer time, we could not reach physiological concentrations in our simulations. [However, because we were well above the percolation threshold, all conclusions reached in this work are practically insensitive to filament concentration above the value 1.56 mg/ml used here (see also Ref. 46).] Cytoskeletal filaments are represented by rigid rods, instead of being semiflexible. [Because the persistence length of F-actin is $>10 \mu\text{m}$ (11), this restriction did not affect our results.] The dynamic nature of the mesh due to constant polymerization and depolymerization of the

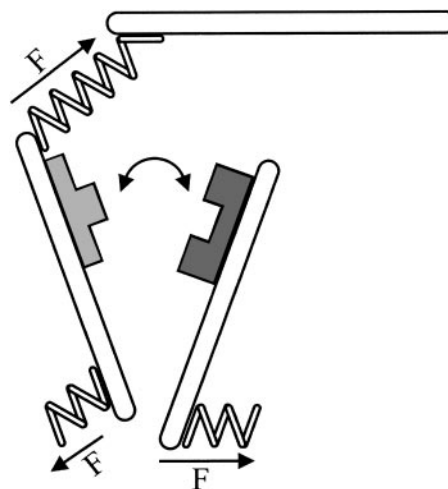


Fig. 7. A possible mechanism for the activation of signaling molecules attached to the cytoskeleton by means of energy propagation along the filaments. The springs linked to the filaments exert forces (F) that move the filaments relative to each other. This in turn causes the cytoskeleton-attached signaling molecules (shaded) to interact and initiate a chemical signaling event.

filaments is not considered. [As found by McGrath et al. (24) for physiological concentrations, the typical turnover time of a cytoskeletal actin filament is around 6 min, which is well above the time our signal reached the nucleus.] Linker molecules are replaced by simple springs. The torsional elasticity of both the filaments and the linkers is not taken into account. More importantly, we have concentrated on one particular pathway: energy propagation along cytoskeletal filaments. We have not included specific biochemical signaling molecules and their interactions. Such complications can, in principle, be incorporated into our computer simulations.

The main objective of the present work was to suggest a specific mechanism for the transduction of mechanical signals to which all living cells are exposed. The main conclusion from our results is that the cytoskeleton can transfer reliably (promptly and without loss of information) external mechanical signals into various parts of the cell (in particular to the nucleus). The presented mechanism is complimentary to conventional biochemical signaling pathways and, because of the intrinsic properties (i.e., stiffness, normal modes) of the filamentous network, supplies another level of cellular control.

We greatly acknowledge useful discussions with D. ben-Avraham.

This work was supported by National Science Foundation Grant IBN-97100010.

REFERENCES

- Banes AJ, Tzuzaki M, Yamamoto J, Fischer T, Brigman B, Brown T, and Miller L. Mechanoreception at the cellular level: detection, interpretation and diversity of responses to mechanical signals. *Biochem Cell Biol* 73: 349–365, 1993.
- Berg HC. *Random Walks in Biology*. Princeton, NJ: Princeton Univ. Press, 1993.
- Bicknese S, Periasamy N, Shohet SB, and Verkman AS. Cytoplasmic viscosity near the cell plasma membrane: measurement by evanescent field frequency-domain microfluorimetry. *Biophys J* 65: 1272–1282, 1993.
- Billeter J and Pelcovits R. Simulations of liquid crystals. *Comput Phys* 12: 440–448, 1998.
- Davies E. Intercellular and intracellular signals and their transduction via the plasma membrane-cytoskeleton interface. *Semin Cell Biol* 4: 139–147, 1993.
- Davis MJ and Hill MA. Signaling mechanisms underlying the vascular myogenic response. *Physiol Rev* 79: 387–423, 1999.
- Davis PE. Flow-mediated endothelial mechanotransduction. *Physiol Rev* 75: 519–560, 1995.
- Dolmetsch E, Lewis RS, Goodnow C, and Healy JL. Differential activation of transcription factors induced by Ca^{2+} response amplitude and duration. *Nature* 386: 855–858, 1997.
- Dong CR, Skalak R, and Sung KL. Cytoplasmic rheology of passive neutrophils. *Biorheology* 28: 557–567, 1991.
- Forgacs G. On the possible role of the cytoskeletal filamentous network in intracellular signaling: an approach based on percolation. *J Cell Sci* 108: 2131–2143, 1995.
- Gittes F, Mickey B, Nettleton J, and Howard J. Flexural rigidity of microtubules and actin filaments measured from thermal fluctuations in shape. *J Cell Biol* 120: 923–934, 1993.
- Goldstein H. *Classical Mechanics*. Reading, MA: Addison-Wesley, 1980.
- Gudi S, Nolan JP, and Frangos JA. Modulation of GTPase activity of G proteins by fluid stress and phospholipid composition. *Proc Natl Acad Sci USA* 95: 2616–2619, 1998.
- Gudi SRP, Lee AA, Clarks A, and Frangos JA. Equibiaxial strain and strain rate stimulate early activation of G proteins in cardiac fibroblasts. *Am J Physiol Cell Physiol* 274: C1424–C1428, 1998.
- Gumbiner BM. Cell adhesion: the molecular basis of tissue architecture and morphogenesis. *Cell* 384: 345–357, 1996.
- Ingber DE. Tensegrity: the architectural basis of cellular mechanotransduction. *Annu Rev Physiol* 59: 575–599, 1991.
- Janney P. The cytoskeleton and cell signaling: component localization and mechanical coupling. *Physiol Rev* 78: 763–781, 1998.
- Juliano RL and Haskill S. Signal transduction from the extracellular matrix. *J Cell Biol* 120: 577–585, 1993.
- Komuro I, Katoh Y, Kaida T, Shibasaki Y, Kurabayashi M, Hoh M, Takaku F, and Yazaki Y. Mechanical loading simulates cell hypertrophy and specific gene expression in cultured rat cardiac myocytes. *J Biol Chem* 266: 1265–1268, 1991.
- Lang I, Scholz M, and Peters R. Molecular mobility and nucleocytoplasmic flux in hepatoma cells. *J Cell Biol* 102: 1183–1190, 1986.
- Liu M, Tanswell AK, and Prost M. Mechanical force-induced signal transduction in lung cells. *Am J Physiol Lung Cell Mol Physiol* 277: L667–L683, 1999.
- Maksym GN, Fabry B, Butler JP, Navajas D, Tschumperlin DJ, Laporte JD, and Fredberg JJ. Mechanical properties of cultured human airway smooth muscle cells from 0.05 to 0.4 Hz. *J Appl Physiol* 89: 1617–1618, 2000.
- Maniotis AJ, Chen CS, and Ingber DE. Demonstration of mechanical connections between integrins, cytoskeletal filaments and nucleoplasm that stabilize nuclear structure. *Proc Natl Acad Sci USA* 94: 849–854, 1997.
- McGrath JL, Tardy Y, Dewey CF Jr, Meister JJ, and Hartwig JH. Simultaneous measurements of actin filament turnover, filament fraction, and monomer diffusion in endothelial cells. *Biophys J* 75: 2070–2078, 1998.
- Millward-Sadler SJ, Wright MO, Lee H, Nishida K, Caldwell H, Nuki G, and Salter DM. Integrin-regulated secretion of interleukin 4: a novel pathway of mechanotransduction in human articular chondrocytes. *J Cell Biol* 145: 183–189, 1999.
- Minoura I, Yagi T, and Kamiya R. Direct measurement of inter-doublet elasticity in flagellar axonemes. *Cell Struct Funct* 24: 27–33, 1999.
- Mochly-Rosen D. Localization of protein kinases by anchoring proteins: a theme on signal transduction. *Science* 268: 247–251, 1995.
- Molloy JE, Burns JE, Sparrow JC, Tregear RT, Kendrick-Jones J, and White DC. Single-molecule mechanics of heavy meromyosin and S1 interacting with rabbit or *Drosophila* actins using optical tweezers. *Biophys J* 68: 298S–305S, 1995.
- Nakamura T, Liu M, Mourgeon E, Slutsky A, and Post M. Mechanical strain and dexamethasone selectively increase surfactant protein C and tropoelastin gene expression. *Am J Physiol Lung Cell Mol Physiol* 278: L974–L980, 2000.
- Naruse K, Yamada T, and Sokabe M. Involvement of SA channels in orienting response of cultured endothelial cells to cyclic stretch. *Am J Physiol Heart Circ Physiol* 274: H1532–H1538, 1998.
- Nicklas RB, Ward SC, and Gorbisky GJ. Kinetochore chemistry is sensitive to tension and may link mitotic forces to a cell cycle checkpoint. *J Cell Biol* 130: 929–939, 1995.
- Numaguchi K, Eguchi S, Yamakawa T, Motley ED, and Inagami T. Mechanotransduction of rat aortic vascular smooth muscle cells requires RhoA and intact actin filaments. *Circ Res* 85: 5–11, 1999.
- Osol G. Mechanotransduction by vascular smooth muscle. *J Vasc Res* 32: 275–292, 1995.
- Ozawa M, Ringwald M, and Kemler R. Uvomorulin-catenin complex formation is regulated by a specific domain in the cytoplasmic region of the cell adhesion molecule. *Proc Natl Acad Sci USA* 87: 4246–4250, 1990.
- Pavalko FM, Chen NX, Turner CH, Burr DB, Atkinson S, Hsieh YF, Qui J, and Duncan RL. Fluid shear-induced mechanical signaling in MC3T3-E1 osteoblasts requires cytoskeleton-integrin interactions. *Am J Physiol Cell Physiol* 275: C1591–C1601, 1998.

36. **Pollard TD, Selden SC, and Maupin P.** Interaction of actin filaments with microtubules. *J Cell Biol* 99: 33s–37s, 1984.
37. **Prahlad V, Yoon M, Moir RD, Vale RD, and Goldman RD.** Rapid movements of vimentin on microtubule tracks: kinesin-dependent assembly of intermediate filament networks. *J Cell Biol* 143: 159–170, 1998.
38. **Rosales C, O'Brien V, Kornberg L, and Juliano R.** Signal transduction by cell adhesion receptors. *Biochim Biophys Acta* 1242: 77–98, 1995.
39. **Rychly J, Pommerenke H, Durr F, Schreiber E, and Nebe B.** Analysis of spatial distributions of cellular molecules during mechanical stressing of cell surface receptors using confocal microscopy. *Cell Biol Int* 22: 7–12, 1998.
40. **Sachs F.** Mechanical transduction by membrane ion channels: a mini review. *Mol Cell Biochem* 104: 57–60, 1991.
41. **Sadosima J and Izumo S.** The cellular and molecular response of cardiac myocytes to mechanical stress. *Annu Rev Physiol* 59: 551–571, 1997.
42. **Sahimi M.** *Applications of Percolation Theory*. London: Taylor and Francis, 1994.
43. **Salter DM, Robb JE, and Wright MO.** Electrophysiological responses of human bone cells to mechanical stimulation: evidence for specific integrin function in mechano-transduction. *J Bone Miner Res* 12: 1133–1141, 1997.
44. **Schmidt C, Pommerenke H, Durr F, Nebe B, and Rychly J.** Mechanical stressing of integrin receptors induces enhanced tyrosine phosphorylation of cytoskeletally anchored proteins. *J Biol Chem* 273: 5081–5085, 1998.
45. **Schmidt FG, Hinner B, Sackmann E, and Tang JX.** Viscoelastic properties of semiflexible filamentous bacteriophage fd. *Phys Rev E Stat Phys Plasmas Fluids Relat Interdiscip Topics* 62: 5509–5517, 2000.
46. **Shafrir Y, ben-Avraham D, and Forgacs G.** Trafficking and signaling through the cytoskeleton: a specific mechanism. *J Cell Sci* 113: 2747–2757, 2000.
47. **Svitkina TM, Verkhovsky AB, and Borisy GG.** Plectin side arms mediate interaction of intermediate filaments with microtubules and other components of the cytoskeleton. *J Cell Biol* 135: 991–1007, 1996.
48. **Toma CD, Ashkar S, Gray ML, Schaffer JL, and Gerstenfeld LC.** Signal transduction of mechanical stimuli is dependent on microfilament integrity: identification of osteopontin as a mechanically induced gene in osteoblasts. *J Bone Miner Res* 12: 1626–1636, 1997.

